Frequency-Dependent Second-Order Hyperpolarizability of Carbon Clusters: A Semiempirical Investigation

Marianna Fanti,† Giorgio Orlandi, and Francesco Zerbetto*

Contribution from the Dipartimento di Chimica "G. Ciamician", Università di Bologna, Via F. Selmi 2, 40126 Bologna, Italy

Received December 9, 1994®

Abstract: Sum over states − complete neglect of differential overlap/spectroscopic parameterization plus configuration interaction, SOS − CNDO/S CI, is used to calculate the dispersion of the second order hyperpolarizability, $\gamma(-3\omega; \omega, \omega, \omega)$ and $\gamma(-2\omega; 0, \omega, \omega)$, of five fullerenes, namely C_{60}, C_{70}, C_{76}, $C_{84}(D_2)$, and $C_{84}(D_{2d})$. Very recent $\gamma(-\omega; \omega, \omega, -\omega)$ dispersion data for C_{60} are also simulated. The five all-carbon molecules studied are available in sufficient quantities to allow for direct experimental measurements. All the Orr Ward diagrams are included in the calculation. Both the real and the imaginary part of the response are calculated. The results show good agreement with the experimentally available data for C_{60} and C_{70}. The calculated static second order hyperpolarizabilities of the five molecules studied scale with the fourth power of the mass of the cluster. At energies lower than the one-photon absorption, the calculated $\gamma(-3\omega; \omega, \omega, \omega)$ dispersion of the five fullerenes shows at least major resonances. The analysis of the differences between computational theory and experiment is used to refine the prediction of the third harmonic generation dispersion of C_{76}, and the two stable isomers of C_{84} for which no experimental data are as yet available. We estimate that the two lowest lying resonances for C_{76} and the two isomers of C_{84} should occur slightly above 1500 and 1100 nm. A "missing state" scheme is used to identify the electronic states responsible for the resonances. The two- and three-photon absorption spectra are also calculated. Further comparison of the calculated $\gamma(-3\omega; \omega, \omega, \omega)$ dispersion with the two- and three-photon simulated spectra together with the calculated $\gamma(-2\omega; 0, \omega, \omega)$ dispersion allows one to fully ascertain the nature of the resonances. The simple picture based on the SOS model limited only to the resonant states is found to account well for the response in the THG dispersion of C_{60}. Such a picture is nearly as successful for C_{70} but fails for higher fullerenes. A source of higher nonlinearity in C_{60} is also explored. This is the possibility of the absorption to S_1 and its subsequent NLO response. The static, off-resonance, $\gamma(0; 0, 0, 0)$ for S_1 and S_2 is found to be an order of magnitude larger than that of S_0.

Introduction

Molecules characterized by an extended conjugated system of carbon atoms possess many attractive attributes that could be exploited to complement traditional nonlinear optical (NLO) materials ($LiNbO_3$ and KH_2PO_4). The usual list of appealing features encompasses ultrafast response times, lower dielectric constants, better processability characteristics, and enhanced NLO responses with respect to the traditional inorganic solids. The search for the optimal carbon-based system for NLO applications is now accelerating also because of the impact of quantum chemical calculations. These computational procedures may serve both as a guide in the prediction of promising materials and allow a deeper insight into the origin of the signal. Amongst the molecules whose investigation might lead to new NLO systems, one should consider carbon clusters[1] whose preparation has now been scaled up to gram size quantities.[2] Their promise lies in the extended conjugation of their π electron systems and in the fact that they do not contain CH bonds whose anharmonic overtones absorb and are therefore detrimental to the NLO response. C_{60} is the prototype of such all-carbon molecules. Its NLO response has been investigated both experimentally and theoretically together with the response of C_{70}.[3−21] Early experimental work determined the propensity of C_{60} for a high NLO response.[5,6,9−17,20] More recent work has emphasized the presence of at least two resonances, possibly of different nature, across the third harmonic generation (THG) dispersion.[17] Quantum chemical predictions and analysis of the NLO properties of C_{60} have been mainly focused on the calculation at zero energy electric field.[6−8,11,13,14] Such calculations are relevant for the far-from-resonance regime. Some

† In partial fullfilment of the requirements of M.F. doctoral's dissertation.

® Abstract published in *Advance ACS Abstracts*, April 15, 1995.

(1) Kroto, H. W.; Heath, J. R.; O'Brien, S. C.; Curl, R. F.; Smalley, R. E. *Nature* **1985**, *318*, 162.

(2) Kraetschmer, W.; Lamb, L. D.; Fostiropoulos, K.; Huffman, D. R. *Nature* **1990**, *347*, 354.

(3) Lindle, J. R.; Pong, R. G. S.; Bartoli, F. J.; Kafafi, Z. H. *Phys. Rev. B* **1993**, *48*, 9447.

(4) Shuai, Z.; Bredas, J. L. *Phys. Rev. B* **1992**, *46*, 16135; **1993**, *48*, 11520.

(5) Wang, Y.; Cheng, L.-T. *J. Phys. Chem.* **1992**, *96*, 1530.

(6) Talapatra, G. B.; Manickam, N.; Samoc, M.; Orczyk, M. E.; Karna, S. P.; Prasad, P. N. *J. Phys. Chem.* **1992**, *96*, 5206.

(7) Matsuzawa, N.; Dixon, D. A. *J. Phys. Chem.* **1992**, *96*, 6241.

(8) Matsuzawa, N.; Dixon, D. A. *J. Phys. Chem.* **1992**, *96*, 6872.

(9) Kafafi, Z. H.; Lindle, J. R.; Pong, R. G. S.; Bartoli, F. J.; Lingg, L. J.; Milliken, J. *Chem. Phys. Lett.* **1992**, *188*, 492.

(10) Meth, J. S.; Vanherzeele, H.; Wang, Y. *Chem. Phys. Lett.* **1992**, *197*, 26.

(11) Li, J.; Feng, J.; Sun, J. *Chem. Phys. Lett.* **1993**, *203*, 560.

(12) Rosker, M. J.; Marcy, H. O.; Chang, T. Y.; Khoury, J. T.; Hansen, K.; Whetten, R. L. *Chem. Phys. Lett.* **1992**, *196*, 427.

(13) Quong, A. A.; Pederson, M. R. *Phys. Rev. B* **1992**, *46*, 12906.

(14) Wang, Y.; Bertsch, G. F.; Tomanek, D. *Z. Phys. D.* **1993**, *25*, 181.

(15) Ji, W.; Tang, S. H.; Xu, G. Q.; Chan, H. S. O.; Ng, S. C.; Ng, W. W. *J. Appl. Phys.* **1993**, *74*, 3669.

(16) Harigaya, K.; Abe, S. *Jpn. J. Appl. Phys.* **1992**, *31*, L235R.

(17) Kajzar, F.; Taliani, C.; Danieli, R.; Rossini, S.; Zamboni, R. *Chem. Phys. Lett.* **1994**, *217*, 418.

(18) Kajzar, F.; Taliani, C.; Danieli, R.; Rossini, S.; Zamboni, R. *Phys. Rev. Lett.* **1994**, *73*, 1617.

(19) Hoshi, H.; Nakamura, N.; Maruyama, Y.; Nakagawa, T.; Suzuki, S.; Shiromaru, H.; Achiba, Y. *Jpn. J. Appl. Phys.* **1991**, *31*, L1397.

(20) Neher, D.; Stegeman, G. I.; Tinker, F. A.; Peyghambarian, N. *Opt. Lett.* **1992**, *17*, 1491.

(21) Yang, S.-C.; Gong, Q.; Xia, Z.; Zou, Y. H.; Wu, Y. Q.; Qiang, D.; Sun, Y. L.; Gu, Z. N. *Appl. Phys. B* **1992**, *55*, 51.

0002-7863/95/1517-6101$09.00/0

calculations of the dispersion have also appeared.[4] C_{70}, the second most abundant carbon cluster, may still be considered at an early stage of the unravelling of its NLO properties from the point of view of both computational theory and experiment. Because of new additional experimental data that are becoming available, both molecules can now be the starting point of a systematic theory able to rationalize the NLO response of these materials. Through a comparison of computational theory with experiment and models, one can assess the deficiencies of the calculations and scale them to produce more reliable predictions. In the present work, we try, first, to summarize some of the previous experimental and computational work connected with carbon clusters and their NLO properties and discuss the best approach to the calculation of such properties. Then, we present the computational scheme for the calculations that we have carried out. Finally, we give our results for C_{60} and C_{70}. Through a comparison with the experimental THG dispersion data of these two molecules, we scale our results and try to formulate an educated estimate of the position of the THG resonances of C_{76} and the two stable isomers of C_{84}. These three molecules are selected because of their availability in sufficient quantities to allow for NLO experiments. The location of the resonances and their characterization allows us to set up simple models which are used to gain further understanding into the NLO properties of these systems. Finally, we investigate $\gamma(0; 0, 0, 0)$ in the two lowest triply degenerate excited states of C_{60}. Notice that, for the sake of immediacy, we have used $\gamma(-2\omega; 0, \omega, \omega)$ and $\gamma(-3\omega; \omega, \omega, \omega)$ and electric field induced second harmonic generation, EFISH, and third harmonic generation, THG, as synonyms. All the calculations reported in this work are microscopic in nature, and no attempt is made to turn them into their macroscopic counterparts.

Experimental and Computational Background

In this work, we are interested in understanding the NLO properties of carbon clusters and in the dynamics, that is frequency dependence, of their second order hyperpolarizabilities, $\gamma(-3\omega, \omega, \omega, \omega)$ and $\gamma(-2\omega; 0, \omega, \omega)$. We shall therefore loosely divide all previous work in two categories: measurements and calculations performed at a selected value of the energy of the incident radiation and measurements and calculations which are frequency dependent. All the previous work deals either with C_{60} or with C_{70}. To the best of our knowledge, the NLO properties of fullerenes larger than C_{70} have not been investigated before either experimentally or theoretically.

In Tables 1 and 2, we present a summary of single frequency experimental and calculated results for C_{60} and C_{70}, respectively. Most of the experimental data were already presented in Tables 1 and 3 in ref 3. THG dispersion curves are reported in ref 17 for C_{60} and in ref 18 for C_{70}. In the tables, the values are given as reported, and no attempt is made here to compare different experiments which were performed under a variety of conditions and in different phases. It is well-known[22] that comparison of experiments and calculations for NLO properties presents difficulties. The calculation is microscopic in nature, the measurement refers to a macroscopic phase in which a number of collective phenomena may play a role. It is not within the scope of this work to investigate this aspect, and, for sake of comparison, we can assume that a factor of $10^{22}-10^{23}$ relates theory and experiment.[22] It is now of interest to focus on the NLO calculations. In general, they employ two different schemes, namely sum over states (SOS) and finite field (FF).

(22) Cheng, L. T.; Tam, W.; Stevenson, S. H.; Meredith, G. R.; Rikken, G.; Marder, S. R. *J. Phys. Chem.* **1991**, *95*, 10631. Cheng, L. T.; Tam, W.; Marder, S. R.; Stiegman, A. E.; Rikken, G.; Spangler, C. W. *J. Phys. Chem.* **1991**, *95*, 10643.

Table 1. Experimental C_{60} Third Order Optical Susceptibility, $\chi^{(3)}$ in esu, and Calculated Second Order Hyperpolarizability, γ in esu

experimental			calculated			
λ (μm)	$\chi 10^{11}$	technique	λ (μm)	$\gamma 10^{34}$	technique	method
0.60	22	DFWM[6]	0	2.041	THF	SOS-VEH[4]
0.63	30	DFWM[12]	0	0.0495		INDO-TDCPHF[6]
0.85	1.5	THF[17]	1.37	0.0504	OKG	INDO-TDCPHF[6]
1.06	0.7	DFWM[9]	1.37	0.0549	EFISH	INDO-TDCPHF[6]
	1.4	THF[10]	1.37	0.0552	DFWM	INDO-TDCPHF[6]
	7.2	THF[20]	0	0.0239		MNDO-PM3[7]
	8.2	THF[17]	0	0.0159		LDA[8]
	20	THF[11]	1.064	8.84	DFWM	SOS-INDO/S[11]
1.32	3.	THF[10]	1.91	6.9	DFWM	SOS-INDO/S[11]
	6.1	THF[17]	0	0.07		LDA[13]
1.50	3.0	THF[20]	0	0.09		TB[14]
1.91	0.9	THF[10]	0	4.58		SOS-CNDO/S[a]
	1.6	EFISH[5]				
	3.2	THF[17]				
2.00	3.7	THF[20]				
2.37	0.4	THF[10]				

[a] Present work.

Table 2. Experimental C_{70} Third Order Optical Susceptibility, $\chi^{(3)}$ in esu, and Calculated Second Order Hyperpolarizability, γ in esu

experimental			calculated			
λ (μm)	$\chi 10^{11}$	technique	λ (μm)	$\gamma 10^{34}$	technique	method
1.06	1.2	DFWM[2]	0	8.937	THF	SOS-VEH[4]
1.42	9	THF[18]	0	0.0452		MNDO-PM3[7]
1.50	54	THG[20]	0	8.57		SOS-CNDO/S[a]
1.91	4.4	EFISH[20]				
2.00	9.1	THG[20]				

[a] This work.

By inspection of Tables 1 and 2, several features become apparent: (i) the experimental results are rather scattered, (ii) the third order optical susceptibility of C_{60} is larger than 10^{-11} esu, (iii) the third order optical susceptibility of C_{70} is larger than that of C_{60}, by, roughly, a factor of two, and (iv) the experimental values are only reproduced by SOS type of calculations.

There may be various reasons for the inaccuracy of FF methods. The most likely is connected with the very low S_0-S_1 energy gap in fullerenes. Whatever the reason, the method of choice to study the NLO properties of carbon clusters should be of the SOS type.

Calculated and experimental dispersion data have been presented in the literature both for C_{60}[4,10,17] and for C_{70}.[4,18] The calculations were performed before the extensive experimental work carried out by Kajzar et al. on the THG of these materials.[17,18] Since little or no fine-tuning of the computational theory with the experiment was done (vide infra), the agreement can be expected to be only qualitative. It is remarkable that, for both molecules, both theory and experiment find a large resonance in the region around 1 eV. More in detail, for C_{60}, comparison of experiment, Figure 2 in ref 17, and theory, Figure 4a in ref 4, shows that the two experimental resonances observed at 1.064 μm (1.17 eV) and 1.3 μm (0.95 eV) are collapsed into one. For C_{70}, the same comparison is a little less flattering in that the experiment[18] shows the most intense resonance at 1.42 μm with a shoulder resonance at 1.00 μm. In this region a total of 44 experimental points were taken[18] and the trend seems to be well established. In the same work,[18] a further THG point was obtained at 1.907 μm, its cross section was found to be due to a nearly-resonant mechanism, and its value was less than that of either of the other two resonances.

This scenario demands further computational investigation of the frequency dependent second order hyperpolarizability of C_{60} and C_{70}. In particular, such calculations can now be critically examined in order to yield an improved prediction of the NLO properties of higher fullerenes.

Computational Procedure

In the previous section, after inspection of the previous results presented in Tables 1 and 2, we have advocated the use of SOS type of calculations for a satisfactory simulation of the order of magnitude of the second order hyperpolarizability. In this section, we present the method we have used.

The quantum chemical model that we employ is the complete neglect of differential overlap/spectroscopic parameterization (CNDO/S).[23] As far as the electronic properties of carbon clusters are concerned, we have found it particularly successful in two tasks. The first is the analysis of the vibronic structure of the S_1-S_0 emission spectrum of C_{60}.[24] The second is the simulation of the circular dichroism spectrum of C_{76}[25] which allowed us to assign the absolute configuration of this chiral molecule. In this latter calculation, we found it to be superior to another, rather similar, molecular Hamiltonian, namely INDO/S, where "I" stands for "intermediate". CNDO/S and INDO/S methods have been widely used to furnish the electronic energies and the transition dipole moments used in the SOS scheme to predict trends in the NLO properties of conjugated molecules. A recent and thorough review of their merits and shortcomings can be found in ref 26.

The calculation of the hyperpolarizabilities is performed using all the Orr Ward diagrams.[27] The first order hyperpolarizability reads

$$\beta_{ijk}(-\omega_3;\omega_1,\omega_2) = K(-\omega_3;\omega_1,\omega_2)\left(\frac{-e^3}{\hbar^2}\right) I_{1,2} \sum_{ab}{}' \left[\frac{r^k_{ga}\bar{r}^i_{ab}r^j_{bg}}{(\omega_{ag}-\omega_3)(\omega_{bg}-\omega_1)} + \frac{r^j_{ga}\bar{r}^i_{ab}r^k_{bg}}{(\omega^*_{ag}+\omega_2)(\omega^*_{bg}+\omega_3)} + \frac{r^j_{ga}\bar{r}^k_{ab}r^i_{bg}}{(\omega^*_{ag}+\omega_2)(\omega_{bg}-\omega_1)} \right] \quad (1)$$

where ω_3 refers to the output radiation and the other ω's to the incident perturbation(s); $K(-\omega_3;\omega_1,\omega_2)$ depends on the nature of the technique used to investigate the NLO properties, $I_{1,2}$ permutates the input radiations, r^i_{ab} is the transition dipole moment between states a and b along the ith axis, and the bar, if present, indicates that the average dipole moment of the initial state along the ith axis has been subtracted, the prime in the summation means that the initial state does not contribute to the sums, and ω_{ag} is the energy difference between the initial state and ath state minus a damping parameter that we have assumed to be 100 cm^{-1} multiplied by the imaginary unit.

For the second order hyperpolarizability, we adopt the general scheme that allows the calculations of excited states γ.[28] This generalized second order hyperpolarizability reads

$$\gamma^{S_n}_{ijkl}(-\omega_4;\omega_1,\omega_2,\omega_3) = K(-\omega_4;\omega_1,\omega_2,\omega_3)\left(\frac{e^4}{\hbar^3}\right) I_{1,2,3} \left[\sum_{abc}{}' \left(\frac{r^j_{nc}\bar{r}^l_{cb}\bar{r}^k_{ba}r^j_{an}}{(\omega_{cn}-\omega_4)(\omega_{bn}-\omega_1-\omega_2)(\omega_{an}-\omega_1)} + \frac{r^l_{nc}\bar{r}^i_{cb}\bar{r}^k_{ba}r^j_{an}}{(\omega^*_{cn}+\omega_3)(\omega_{bn}-\omega_1-\omega_2)(\omega_{an}-\omega_1)} + \frac{r^j_{nc}\bar{r}^k_{cb}\bar{r}^i_{ba}r^l_{an}}{(\omega^*_{cn}+\omega_1)(\omega^*_{bn}+\omega_1+\omega_2)(\omega_{an}-\omega_3)} + \frac{r^j_{nc}\bar{r}^k_{cb}\bar{r}^l_{ba}r^i_{an}}{(\omega^*_{cn}+\omega_1)(\omega^*_{bn}+\omega_1+\omega_2)(\omega^*_{an}+\omega_4)} \right) - \sum_{ab}{}' \left(\frac{r^{i1}_{nb}r^l_{bn}r^k_{na}r^j_{an}}{(\omega_{bn}-\omega_4)(\omega_{bn}-\omega_3)(\omega_{an}-\omega_1)} + \frac{r^i_{nb}r^l_{bn}r^k_{na}r^j_{an}}{(\omega_{bn}-\omega_3)(\omega^*_{an}+\omega_2)(\omega_{an}-\omega_1)} + \frac{r^l_{nb}r^i_{bn}r^j_{na}r^k_{an}}{(\omega^*_{bn}+\omega_4)(\omega^*_{bn}+\omega_3)(\omega^*_{an}+\omega_1)} + \frac{r^l_{nb}r^i_{bn}r^j_{na}r^k_{an}}{(\omega^*_{bn}+\omega_3)(\omega_{an}-\omega_2)(\omega^*_{an}+\omega_1)} \right) \right] \quad (2)$$

A more direct comparison with experiment is possible through $\langle\gamma\rangle$ which reads

$$\langle\gamma\rangle = (\gamma_R^2 + \gamma_I^2)^{1/2} \quad (3)$$

where R and I are the real and the imaginary components and

$$\gamma_S = \frac{1}{5}\left[\frac{1}{3}\left(\sum_{i\neq j}(\gamma_{iiij}+\gamma_{ijji}+\gamma_{ijij})\right) + \gamma_{xxxx} + \gamma_{yyyy} + \gamma_{zzzz}\right] \quad (4)$$

s stands for the real or the imaginary part.

To make the presentation of the results more pleasing to the eye, the stick spectrum obtained from the calculations, i.e., energies and cross sections, is then broadened by multiplying it by a function $G(\nu)$,

$$G(\nu) = \frac{e^{-(\nu-\nu 0)^2/a^2}}{(a^*\pi^{0.5})} \quad (5)$$

where ν is the wavenumber of the incident radiation, in cm^{-1}, ν_0 is the wavenumber at which the NLO calculation was performed, in cm^{-1}, and a is a constant, in cm^{-1}.

A further tool that may be valuable in the assessment of the origin of the resonances in the dispersion is the calculation of the two- and three-photon absorption cross sections. The two-photon intensity reads[29,30]

$$B \propto \sum_{i,j}(S^s_{ii}S^s_{jj} + 7S^s_{ij}S^s_{jj}) \quad (6)$$

where

$$S^{gf}_{ij} = \left(\frac{e^2}{\hbar^2}\right)\sum_a{}' \left[\frac{r^i_{ga}r^j_{af}}{(\omega_{ag}-\omega)} + \frac{r^i_{fa}r^j_{ag}}{(\omega_{ag}-\omega)} \right] \quad (7)$$

(23) Del Bene, J.; Jaffè, H. H. *J. Chem. Phys.* **1968**, *48*, 1807. Nishimoto, K.; Mataga, N. *Z. Physik. Chem.* **1957**, *13*, 140.
(24) Negri, F.; Orlandi, G.; Zerbetto, F. *J. Chem. Phys.* **1992**, *97*, 6496.
(25) Poggi, G.; Orlandi, G.; Zerbetto, F. *Chem. Phys. Lett.* **1994**, *224*, 113.
(26) Kanis, D. R.; Ratner, M. A.; Marks, T. J. *Chem. Rev.* **1994**, *94*, 195.
(27) Orr, B. J.; Ward, J. F. *Mol. Phys.* **1971**, *20*, 513.
(28) Zhou, Q. L.; Heflin, J. R.; Wong, K. Y.; Zamani-Khamiri, O.; Garito, A. F. *Phys. Rev. A* **1991**, *43*, 1673.

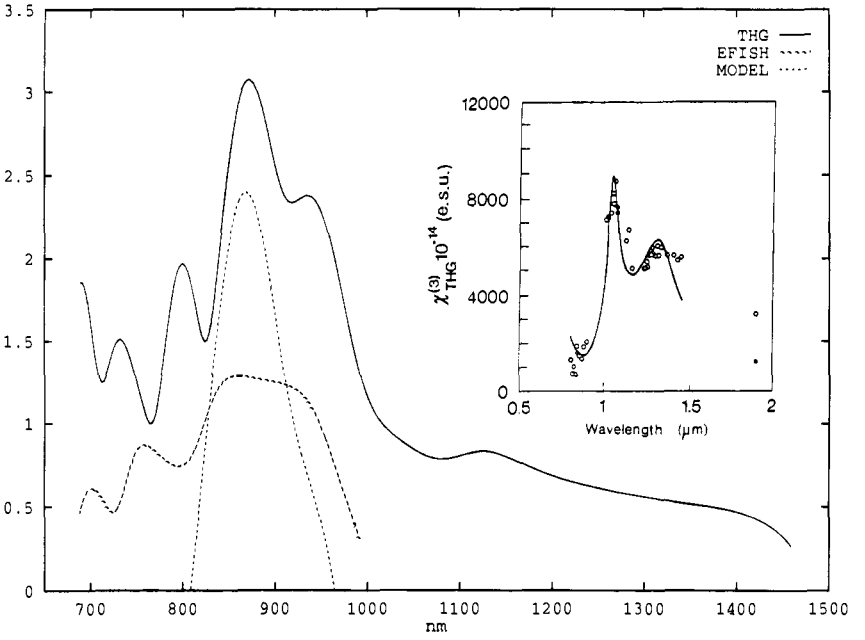

Figure 1. Logarithm of the frequency dependent NLO dispersion of C_{60}. The full line is the SOS CNDO/S CI calculated $\gamma(-3\omega; \omega, \omega, \omega)$; the dashed line is the SOS CNDO/S CI calculated $\gamma(-2\omega; \omega, \omega, \omega)$; the short dashed line is resonant-states modeled $\gamma(-3\omega; \omega, \omega, \omega)$ (see text). The line width, a, is 350 cm^{-1}. The inset shows the experimental results of ref 17.

the three-photon intensity reads[29-31]

$$I \propto \sum_{i,j,k} (T^s_{ijj} T^s_{ikk} + 3T^s_{ijk} T^s_{ikk}) \tag{8}$$

where

$$T^{gf}_{ijk} = \left(\frac{-e^3}{\hbar^2}\right) \sum_{ab}{}' \frac{r^i_{fa} r^j_{ab} r^k_{bf}}{(\omega_{ag} - 2\omega)(\omega_{bg} - \omega)} \tag{9}$$

The simulated two- and three-photon spectra together with the THG and EFISH frequency dependent calculations allow for a clear picture of the nature of the resonances.

Results and Discussion

The Cartesian coordinates of the carbon clusters were first optimized with the QCFF/PI model[32] which was shown to yield accurate results for fullerenes.[33] A set of exploratory calculations was performed with a configuration interaction of 197 electronic states (all the singly excited configurations from the space of 14 occupied molecular orbitals to 14 unoccupied molecular orbitals). Soon it became apparent that this molecular orbital space is too small to obtain meaningful results for the molecules at hand. The main reason for this lies in the fact that this amount of CI gives a highest excitation energy well below the threshold of three times the S_0-S_1 transition (vide infra). We therefore decided to use a 31*31 configuration interaction for all the systems studied here. There was one exception that is C_{60} whose high symmetry forced us to use a 28*30 MO space. The SOS procedure included all the electronic states below 7.0 eV. With this threshold and since, in these molecules, the calculated S_0-S_1 excitation energy is about 2 eV, all the electronic states that may be up to three-photon resonant in THG dispersion are accounted for. In principle, a configuration interaction scheme limited to singly excited configurations might not suffice to describe the second order hyperpolarizability. However, the necessity of including all the states that might be resonant in THG would make the number of electronic states in the SOS calculation too large to handle on any computer. In the light of previous work that showed that, for fullerenes, inclusion of doubly excited configurations does not alter the results obtained only with the single excitations,[11] we decided to limit our CI to singles. It is the ability of the calculations to simulate the experimental results that is called upon to evaluate their accuracy.

Table 3. Calculated Static Second Order Hyperpolarizabilities, esu *10^{34}

	C_{60}	C_{70}	C_{76}	$C_{84}(D_2)$	$C_{84}(D_{2d})$
γ_{xxxx}	−4.58	−8.43	−14.40	−21.83	−15.67
γ_{yyyy}	−4.58	−8.43	−13.44	−18.58	−19.07
γ_{zzzz}	−4.58	−10.12	−9.11	−14.17	−19.07
γ_{xxyy}, γ_{yyxx}	−1.53	−2.81	−4.16	−6.78	−5.90
γ_{xxzz}, γ_{zzxx}	−1.53	−2.55	−4.04	−5.69	−5.90
γ_{yyzz}, γ_{zzyy}	−1.53	−2.55	−3.64	−5.54	−6.29
γ_{yxxy}, γ_{xyyx}	−3.47	−6.52	−1.02	−15.28	−13.20
γ_{yzzy}, γ_{zyyz}	−3.47	−6.59	−8.43	−12.44	−14.26
γ_{xzzx}, γ_{zxxz}	−3.47	−6.59	−9.04	−13.05	−13.20
γ_{xyxy}, γ_{yxyx}	0.41	0.90	1.90	1.73	1.40
γ_{zxzx}, γ_{xzxz}	0.41	1.49	0.95	1.70	1.40
γ_{zyzy}, γ_{yzyz}	0.41	1.49	1.14	1.37	1.67
$\langle\gamma\rangle$	−4.58	−8.57	−12.13	−18.12	−18.00

In Table 3, we show the components of the static second order hyperpolarizabilities for the five molecules studied here. Our program does not enforce symmetry, however, standard symmetry relations between the tensor components are satisfied. Amongst them, worth mentioning, is the relation $\gamma_{xxxx} = \gamma_{xxyy} + \gamma_{xyyx} + \gamma_{xyxy}$ which holds for the I_h point group symmetry. From the table, it is seen that the larger the number of carbon atoms, the higher the static response. If one assumes the $\langle\gamma\rangle$ value of C_{60} as a reference, the results scale as the fourth power of the ratio of the number of atoms divided by 60, $(n/60)^4$: in practice, this fourth power law gives $\langle\gamma_{C_{70}}\rangle = -8.48*10^{-34}$ esu

(29) Andrews, D. L.; Ghoul, W. A. *J. Chem. Phys.* **1981**, *75*, 530.
(30) Marchese, F. T.; Jaffè, H. H.; Seliskar, C. J. *J. Chem. Phys.* **1980**, *72*, 4194.
(31) Grubb, S. G.; Otis, C. E., Haber, K. S.; Albrecht, A. C. *J. Chem. Phys.* **1984**, *81*, 5255.
(32) Warshel, A.; Karplus, M. *J. Am. Chem. Soc.* **1972**, *94*, 5612.
(33) Orlandi, G.; Zerbetto, F.; Fowler, P. W.; Manolopoulos, D. E. *Chem. Phys. Lett.* **1993**, *208*, 441.

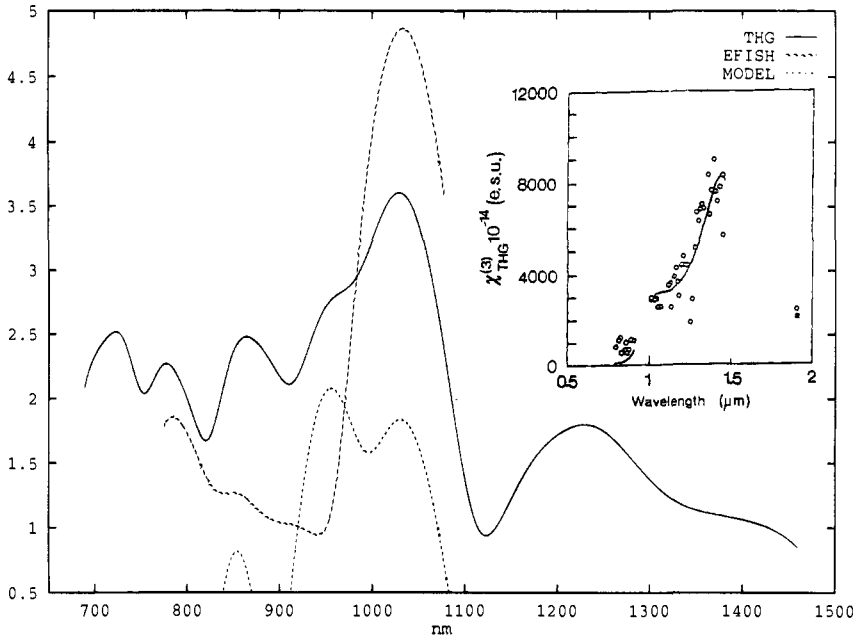

Figure 2. Logarithm of the frequency dependent NLO dispersion of C_{70}. The full line is the SOS CNDO/S CI calculated $\gamma(-3\omega; \omega, \omega, \omega)$; the dashed line is the SOS CNDO/S CI calculated $\gamma(-2\omega; \omega, \omega, \omega)$; the short dashed line is resonant-states modeled $\gamma(-3\omega; \omega, \omega, \omega)$ (see text). The line width, a, is 350 cm^{-1}. The inset shows the experimental results of ref 18.

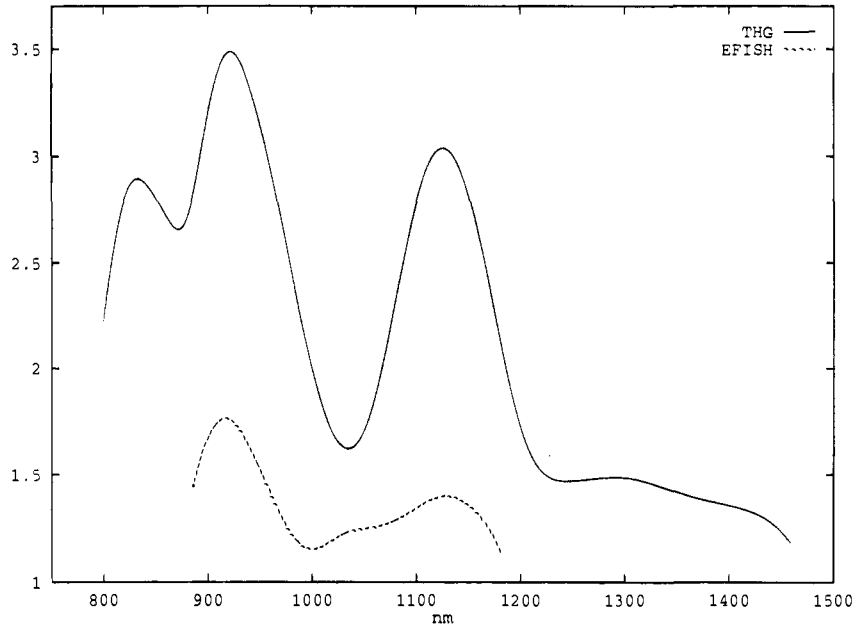

Figure 3. Logarithm of the frequency dependent NLO dispersion of C_{76}. The full line is the SOS CNDO/S CI calculated $\gamma(-3\omega; \omega, \omega, \omega)$; the dashed line is the SOS CNDO/S CI calculated $\gamma(-2\omega; \omega, \omega, \omega)$. The line width, a, is 350 cm^{-1}.

vs a calculated value of $-8.57*10^{-34}$ esu; $\langle\gamma_{C_{76}}\rangle = -11.79*10^{-34}$ esu vs a calculated value of $-12.13*10^{-34}$ esu; $\langle\gamma_{C_{84}}\rangle = -17.59*10^{-34}$ esu vs calculated values of $-18.12*10^{-34}$ and $-18.00*10^{-34}$ esu for the two isomers. One can conclude that the possible interference effects brought about by the additional carbon atoms and by the reduced symmetry are negligible when compared to the cluster size increase which makes for larger transition dipole moments and lower transition energies. Our ability to find this power law also tells us that the present level of calculations treated the five fullerenes in a consistent way.

Interestingly, the calculated values for $\beta_{vect}(0; 0, 0)$ for C_{76}, $C_{84}(D_2)$, and $C_{84}(D_{2d})$ are $6.22*10^{-38}$ esu, $6.04*10^{-35}$ esu, and $5.16*10^{-34}$ esu. Although only these three molecules have nonzero β_{vect}, it is evident that this quantity does not scale with the cluster mass. Its value, instead, increases by lowering the spherical degree of the cluster. Notice that the present calculation does not deal with the magnetic or the quadrupolar components which are deemed to be the origin of the nonzero β_{vect} in C_{60}.[34]

In Figures 1−5, we show the calculated $\gamma(-3\omega; \omega, \omega)$ and $\gamma(-2\omega; 0, \omega, \omega)$, dispersions calculated for a grid of points. The corresponding values are provided in the supplementary material where, for C_{60}, we also provide similar results for the dispersion of $\gamma(-\omega; \omega, \omega, -\omega)$. The EFISH values are calculated in the region of the THG resonances to assist in the process of ascertaining their nature. In these calculations, we only evaluate the sum of diagonal tensor elements. Therefore, one can ascribe a semiquantitative value to the calculated response.

(34) Shuai, Z.; Bredas, J. L. *Adv. Mater.* **1994**, *6*, 486.

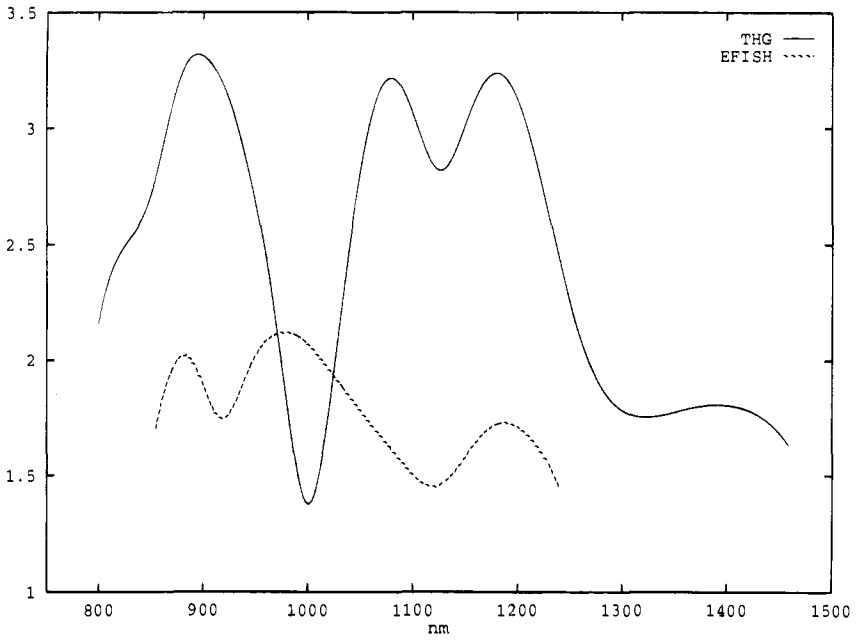

Figure 4. Logarithm of the frequency dependent NLO dispersion of $C_{84}(D_2)$. The full line is the SOS CNDO/S CI calculated $\gamma(-3\omega; \omega, \omega, \omega)$; the dashed line is the SOS CNDO/S CI calculated $\gamma(-2\omega; \omega, \omega, \omega)$. The line width, a, is 350 cm^{-1}.

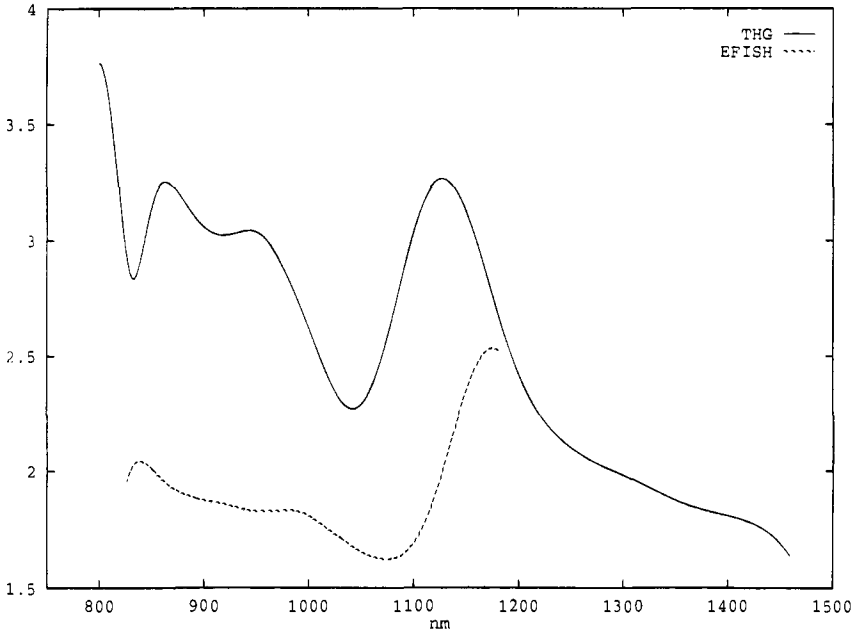

Figure 5. Logarithm of the frequency dependent NLO dispersion of $C_{84}(D_{2d})$. The full line is the SOS CNDO/S CI calculated $\gamma(-3\omega; \omega, \omega, \omega)$; the dashed line is the SOS CNDO/S CI calculated $\gamma(-2\omega; \omega, \omega, \omega)$. The line width, a, is 350 cm^{-1}.

Comparison of Figures 1−5 shows that all the clusters studied here possess at least two resonances below the one-photon absorption. Moreover, although different in cross section, the resonances of C_{76} and the two C_{84} isomers are calculated at similar energies.

The presence of two resonances, for the smaller fullerenes, agrees well with the experimental results of Kajzar et al.[17,18] They were located at 1300 and 1064 nm for C_{60} and at 1420 and 1000 nm for C_{70}. The grid calculations yielded resonances at 936 and 870 nm for C_{60} and 1033 and 855 nm for C_{70}. It appears that the present calculations give a systematic inaccuracy of the order of 2000−2500 cm^{-1}. We can therefore formulate an experimentally-educated theoretical estimate of the position of the two low lying resonances in C_{76} and C_{84}. Since the calculations give them above 1100 and above 900 nm, in the real molecules, they should occur around 1400 and 1100 nm, respectively.

Before going into some detail about the nature of the resonances, one should be aware of the fact that the THG resonances can have a two-photon component even though they do not appear as resonances in the EFISH calculations. In such a case, the numerator of eq 2 plays a major role. To establish the nature of the resonance more firmly, we also calculated the one-, two-, and three-photon intensities for the electronic transitions of the five molecules studied here. The results are shown in Tables 6−10 of the supplementary material. As a further tool to unravel the origin of the resonances, we adopted a "missing state" scheme by which an electronic state deemed to cause a resonance is entirely removed from the SOS procedure. Repeated application of this scheme allowed us to obtain a good insight into our computational results. Before examining in detail the position of the resonances and their nature, we should mention that the energy of the photon reported below refers to the grid calculation, while the resonance is

located exactly by diagonalization of the configuration interaction matrix. We find this way of presenting the results less confusing than giving a set of irregularly spaced energies.

The dispersion of C_{60} is shown in Figure 1 together with the EFISH dispersion and the THG modeling with reduced dimensionality (vide infra). The grid calculations find that the imaginary THG component peaks at 1.325 and at 1.425 eV. Removal, in the SOS procedure, of the H_g state at 2.65 eV, makes the response drop from $35.10*10^{-34}$ esu to $11.04*10^{-34}$ esu. This state is two-photon active in the transition from the ground state. Because of the lack of a resonance, at this energy, in the EFISH calculations, we can also gather that this is not a true two-photon resonance although a two-photon transition is promoting it. The second resonance is at 1.425 eV. The missing state procedure successfully decreased the response from $92.83*10^{-34}$ to $3.97*10^{-34}$ esu when we removed the T_{1u} state at 4.29 eV. This state is very active in the one-photon transition from S_0 and only weakly active in the three-photon transition. Overall there is very good agreement between Figure 1 and the dispersion data reported in ref 17 that are also shown in the inset of the figure. The ability of the present calculations to simulate the second order hyperpolarizability can also be assessed against the DFWM experimental results reported by Strohkendl et al. in ref 35. In that work, it is shown that, in the range between 1.42 eV (875 nm) and 1.66 eV (745 nm), the response of C_{60} has two major characteristics: first, it decreases monotonically with the increasing energy of the radiation, and second, it has a sizeable imaginary component. If one accounts for a systematic overestimate of the calculated energy by 0.3−0.4 eV (vide supra), these experimental result corresponds to the range between 1.70 and 1.85 eV. In fact, the calculated $\gamma(-\omega; \omega, \omega, -\omega)$ is $5.97*10^{-34}$ esu at 1.75 eV (with an imaginary component of less than $0.01*10^{-34}$ esu), $5.56*10^{-34}$ esu at 1.80 eV (with an imaginary component of $-0.32*10^{-34}$ esu), and $4.24*10^{-34}$ esu at 1.85 eV (with an imaginary component of $-0.41*10^{-34}$ esu). The qualitative agreement with the experimental trend is very satisfactory and further confirms the validity of the present computational scheme.

In C_{70}, the first resonance occurs at 1.20 eV. Its activity is due to the two-photon transition to the first totally symmetric state located at 2.40 eV. Its removal yields a THG response of $0.94*10^{-33}$ esu versus the calculated value of $20.72*10^{-33}$ esu. This is a true two-photon resonance. In fact, this state is also responsible for a large EFISH resonance (see Figure 2). Amongst all the fullerenes examined by us, this was the only real EFISH resonance that we found. Two smaller resonances are calculated at 1.30 and 1.45 eV. The first owes its activity to the A_2'' state at 3.91 eV which is reasonably strong both in one- and in three-photon transitions. The second resonance at 1.45 eV owes its activity to the A_2'' state located at 4.35 eV. This activity is due to an intense one-photon transition dipole moment. Overall there is very good agreement with the dispersion data of Figure 2 and those reported in ref 18 that are also shown in the inset of the figure.

In C_{76}, the first resonance is located at 1.10 eV. Analogously to C_{70}, it is caused by the first totally symmetric excited state at 2.21 eV. Without this state, the THG value drops from $11.87*10^{-33}$ to $0.98*10^{-33}$ esu. This state has a large two-photon transition dipole moment from S_0. The second resonance at 1.35 eV is due to a mixture of two- and three-photon transitions. The removal of the A state at 2.71 eV lowers the response from $16.76*10^{-33}$ to $4.77*10^{-33}$ esu, while the removal of the B_3 state at 4.05 eV gives a response of $8.20*10^{-33}$ esu. The dispersion curve is shown in Figure 3.

In $C_{84}(D_2)$, the first resonance is found at 1.05 eV. The missing state calculation without the A state located at 2.10 eV gives a THG response of $6.04*10^{-33}$ esu, against a calculated value of $14.18*10^{-33}$ esu. The second resonance is calculated at 1.15 eV and is due to the A state at 2.34 eV. Without this state, the THG value goes from $14.05*10^{-33}$ to $0.76*10^{-33}$ esu. The third resonance is at 1.40 eV and is caused by the A state at 2.67 eV. When this state is removed, the THG response drops from $12.37*10^{-33}$ to $0.65*10^{-33}$ esu. By symmetry, the A states can only be two- and three-photon active.

Interestingly, the resonances of $C_{84}(D_{2d})$ differ rather markedly from those of $C_{84}(D_2)$ in particular and those of the other fullerenes in general. Both the resonances we found are one- or three-photon in nature. The 1.10 eV resonance is promoted by the E state at 3.29 eV, while the 1.45 eV resonance is caused by the E state at 4.34 eV. In our missing state analysis, we also found that the 1.10 eV resonance is depressed by the B_2 state at 3.31 eV. The activity of such an antiresonance becomes apparent if one first notices that this state is actually the cause of the large γ_{xxxx} negative value at 1.10 eV. However, since the other diagonal tensor elements are positive, suppression of this state actually enhances the response.

The first resonance of all the fullerenes studied here except one is promoted by a virtual two-photon transition from S_0. The one exception is $C_{84}(D_{2d})$ whose initial virtual transition is one- or three-photon in nature. For the second resonance, the description is more complicated. In C_{60} and C_{70}, we can confidently assign the initial transition to a one-photon S_0-S_n transition. In C_{76} and $C_{84}(D_2)$ it is a mixture of two- and three-photon transitions. $C_{84}(D_{2d})$ seems to be a case on its own.

It is tempting now to try and find if the response of these systems can be modeled by just a few electronic states. We have attempted such modeling by repeating the SOS calculations with just the resonant electronic states. We did not attempt to reproduce the dispersion data represented in Figures 1−5 as such. Instead, we tried to validate the hypothesis that the whole dispersion could be described by a few level model. For the high symmetry cases, namely C_{60} and C_{70}, the modeling was rather successful (see Figures 1 and 2). For the other three molecules, the SOS procedure limited to the resonant states accounted for far less than 10% of the whole dispersion.

A final point to address is the suitability of these materials for excited state NLO. Although the possibility of a two-photon excitation followed by NLO phenomena has been implied before for C_{60},[3] this topic is of more general interest. In reality, the excited state can be generated also and, more likely, by a single photon process of the adequate energy. Because of the lack of experimental data, we focus onto C_{60} only, and we simply calculate its static γ. Although it is now clear that in hydrocarbon matrix the first excited state of C_{60} is of T_{1g} symmetry,[24] it is of more general interest to calculate the response for the two lowest, nearly degenerate, electronically excited states, i.e., T_{2g} and T_{1g}. For each of the three components of the T_{2g} electronic state, the calculated response is $5.10*10^{-33}$ esu, while for each of the three components of the T_{2g} electronic state, the calculated response is $-2.80*10^{-33}$ esu. The static γ response of C_{60} is therefore about ten times as large as that of C_{60} itself in the ground electronic state. Such response is at least as large as the largest fullerene studied here.

Conclusion

We have attempted a rather general modeling of the NLO properties of fullerenes. The validity of the present, somewhat limited, although computationally intensive, semiempirical treatment is strongly supported by the agreement between

calculated and experimental THG dispersion data of C_{60}[17] and C_{70}[18] and DFWM dispersion data of C_{60}.[35] All the fullerenes modeled here have been actually isolated experimentally and are available in sufficient quantities to allow NLO measurements. By hindsight, it is probably fair to say that C_{60} remains the most intriguing of the materials studied here. Its static γ value can be used as a reference for a simple power law that gives the corresponding values of C_{70}, C_{76}, and the two isomers of C_{84}. Similar power laws have been found for polyenes,[36] but to the best of our knowledge it is the first time that they are proposed for fullerenes. It also shows the two major resonances which are, by and large, shown by the other fullerenes. The first of these resonances is two-photon in nature, although it is not EFISH active, the second is one- or three-photon active. Important counterexamples to the C_{60} behavior are the first and, for practical purposes, the only resonance of C_{70} which is a true two-photon, EFISH active, resonance and $C_{84}(D_{2d})$ which is a case in its own right in that neither of its resonances has a two-photon character and its lowest resonance has some anti resonance character. C_{60} and, to lesser extent, C_{70}, are also amenable to modeling of the THG dispersion with a low dimensional scheme in which only the resonant states are used in the sum over states. Finally, we have shown that once C_{60} is excited to the first electronically excited state, its static γ value is at least as large as that of the largest fullerene studied here.

Acknowledgment. We are grateful to all the authors of ref 17 and 18 for preprints of their work and to one of the referees for drawing our attention to ref 35.

Supplementary Material Available: Tables 1−5 contain the calculated grids of points of $\gamma(-3\omega; \omega, \omega, \omega)$, $\gamma(-2\omega; 0, \omega, \omega)$ for the five isomers and for C_{60} also $\gamma(-\omega; \omega, \omega, -\omega)$ dispersion, Tables 6−10 contain the electronically excited state symmetries, energies, and S_0-S_n one-photon, M, two-photon, B, and three-photon, T, transition dipole moments for the five isomers (All the states below 4.5 eV are given), and Table 11 contains the calculated static second order hyperpolarizabilities for the first two electronically excited states of C_{60} (27 pages). This material is contained in many libraries on microfiche, immediately follows this article in the microfilm version of the journal, can be ordered from the ACS, and can be downloaded from the Internet; see any current masthead page for ordering information and Internet access instructions.

JA943975Q

(35) Strohkendl, F. P.; Larsen, R. J.; Dalton, L. R.; Hellwarth, R. W.; Sarkas, H. W.; Kafafi, Z. H. *SPIE Proceedings* **1994**, *2284*, 78.

(36) Samuel, I. D. W.; Ledoux, I.; Dhenaut, C.; Zyss, J.; Fox, H. H.; Schrock, R. R.; Silbey, R. J. *Science* **1994**, *265*, 1070.